

The Evaluation of MAPK/ERK Signaling Pathway in Chicken Necrotic Enteritis Based on Microbiomics and Metabolomics

Changqin XIE^{ID}, Liyue SUN^{ID}, Yanyi LI^{ID}, Yuting CHU^{ID}, Xiaoli Liu^{ID}, Qingping Tong^{ID}, and Changqin GU*^{ID}

College of Veterinary Medicine, Huazhong Agricultural University, Wuhan 430070, Hubei, China 2 Wuhan Cineda Biological Co., Ltd., Xianning 437222, Hubei, China

*Corresponding author's E-mail: guchangqin@mail.hzau.edu.cn

Received: March 14, 2025, Revised: April 17, 2025, Accepted: May 21, 2025, Published: June 25, 2025

ABSTRACT

Chicken necrotic enteritis is a prevalent intestinal disease caused by *Clostridium perfringens* (*C. perfringens*) in chickens. Previous research has confirmed the close relationship between the gut microbiota and its metabolites in connection with chicken necrotic enteritis. However, it remains unclear how the gut microbiota of the host influences host metabolism following the onset of necrotic enteritis (NE). The close relationship between gut microbiota and their metabolites in chicken necrotic enteritis (NE) has been established, yet the metabolic influence of microbiota post-NE onset remains unclear. In this study, 1-day-old White Leghorn chickens were divided into three groups (n=10/group), a negative control (CON) fed a basal diet, a fishmeal-supplemented group (F) receiving 50% fishmeal, and an NE group inoculated orally with *C. perfringens* alongside fishmeal supplementation. Growth performance, intestinal lesions, and morphological changes were recorded. Cecal contents were subjected to 16S rDNA sequencing for microbiota profiling, while serum metabolomics was analyzed via LC-MS. No noticeable damage was observed in the small intestines of the F group, whereas the NE group exhibited marked body weight reduction. Cell necrosis and jejunal mucosal shedding were identified, accompanied by ileal villi atrophy and significant reductions in tight junction proteins (Claudin-1 and ZO-1). Both F and NE groups showed decreased cecal abundances of *Lactobacillus* and *Blautia*, alongside increased *Clostridium* and *Escherichia coli*. Serum metabolomics revealed distinct glycerophospholipid and arginine-proline metabolism alterations in the F group versus CON. In contrast, NE-associated metabolic shifts were linked to pathways regulating cell proliferation, differentiation, and migration, particularly MAPK signaling. Downregulation of MAPK/ERK pathway genes was detected in the jejunal mucosa of infected chickens compared to CON and F groups. Concurrently, jejunal PCNA expression was quantified and found to be significantly reduced in the NE cohort relative to controls. Drawing upon the experimental results, it was concluded that necrotic enteritis in chickens was linked to a disruption in the intestinal epithelial barrier. Additionally, alterations in the gut microbiota hindered the activation of the MAPK/ERK signaling pathway, which in turn reduced the proliferation of intestinal epithelial cells and impaired the repair processes crucial for intestinal barrier restoration.

Keywords: Chicken, Necrotic enteritis, Microbiomics, Metabolomics, MAPK/ERK, Signaling pathway

INTRODUCTION

Necrotic enteritis (NE) in chickens, caused by *Clostridium perfringens* (*C. perfringens*), is a common disease in the poultry industry, often leading to significant economic losses (Skinner et al., 2010; Timbermont et al., 2010). NE has both clinical and subclinical forms. The clinical variant is characterized by sudden onset and high mortality rates, sometimes reaching 50% (Lee and Lillehoj, 2022; Timbermont et al., 2011), while the subclinical form primarily results in chronic intestinal mucosal damage in

chickens, leading to nutrient malabsorption, lower growth rates, and inefficient feed consumption (Caly et al., 2015).

The development of NE requires predisposing factors, as infection with *C. perfringens* alone is often insufficient to induce the disease. The addition of high concentrations of fish meal in the feed is a major factor in the development of NE in chickens, as it supplies the nutrients required for the proliferation of CP (Drew et al., 2004a; Wu et al., 2010). It has also been shown that a diet exclusively consisting of fishmeal, when combined with a *C. perfringens* infection, leads to substantial alterations in

the intestinal microbiota of chickens (Stanley et al., 2014). The intestinal flora actively participates in the regulation of numerous metabolic processes, including the metabolism of fatty acids, carbohydrates, and amino acids, and it closely interacts with the host's nutritional metabolism (Eckel, 2021). Metabolomic studies on hens with necrotic enteritis have primarily focused on the metabolites of gut microbiota, highlighting alterations in compounds such as bile acids, amino acids, and short-chain fatty acids (Bansal et al., 2020; Kidd et al., 2021; Wang et al., 2021a; Zaytsoff et al., 2022). Additionally, research using integrated metabolomics and transcriptomics analysis has revealed a strong correlation between intestinal damage in hens suffering from necrotic enteritis and the c-Jun N-terminal kinase (JNK) signaling pathway (Xiao, 2022). However, very few studies have delved into changes in serum metabolism and how it relates to gut flora in NE-affected chickens. Investigating the relationship between serum metabolites and gut microbiota can elucidate the systemic metabolic effects of NE, offering a more comprehensive understanding of its pathology and providing a clearer insight into the underlying disease mechanisms. This study aims to identify the potential mechanisms of NE in chickens, providing insights for its treatment. A NE model was established to analyze changes in the intestinal mechanical and chemical barriers, microbiota, and serum metabolomics following NE. Differential metabolites were identified, and altered metabolic pathways were constructed to elucidate the mechanisms of NE, offering valuable references for its treatment.

MATERIALS AND METHODS

Ethical approval

The animal use protocol in this study was approved by the Huazhong Agricultural University Animal Protection and Use Committee, located in Wuhan, China (Permit number: HZAUCH-2023-0009).

Bacterial strains

The *C. perfringens* type G strain was isolated from the liver of chickens naturally infected with NE and preserved by the laboratory of the Veterinary Pathology, Huazhong Agricultural University, Wuhan, China.

Animal experiment design and basal diet

Thirty one-day-old white Leghorn chickens with an average weight of 35.1 ± 1.57 g was procured from Beijing Boehringer Ingelheim Vital Biotechnology Co., Ltd., situated in Beijing, China. Chickens are 15 males and 15

females. These one-day-old chickens were divided into three groups at random, each with ten chickens including the negative control group (CON), chickens were given basic feed; fish meal group (F), chickens were given high fish meal feed; infected group (NE), chickens were given high fish meal feed and gavaged with *C. perfringens*. From day 1 to day 14, all groups were fed a basic diet (Figure 1). From day 15 to day 23, groups F and NE were fed a high fishmeal diet. From day 19 to day 23, chickens in group NE were given 5×10^8 to 5×10^9 CFU of *C. perfringens* orally, while chickens in groups CON and F were given comparable amounts of sterile Fluid Thioglycollate (FTG) medium orally. The trial lasted for 24 days. Throughout the trial, the chickens were kept in wire cages with a 12-hour light cycle and unlimited access to food and water. The composition of the basal diet is shown in Table 1. And the vaccination and prevention protocols was shown in Table 2.

	1d	14d	19d	23d
Group CON		basic diet	basic diet-FTG	
Group F	basic diet	50% Fishmeal	50% Fishmeal-FTG	
Group NE	basic diet	50% Fishmeal	50% Fishmeal- <i>C. perfringens</i>	

Figure 1. The experimental design of the present study. Group CON (n=10): *C. perfringens* -uninfected chickens with basic diet; Group F (n=10): *C. perfringens* uninfected chickens with high fishmeal diet; Group NE (n=10): *C. perfringens* -infected chickens with high fishmeal diet.

Table 1. Guaranteed analytical value of product

Components:	Content (%)
Moisture: ≤	14.0
Crude protein: ≥	20.00
Calcium:	0.60-1.20
Total phosphorus: ≥	0.50
Sodium chloride:	0.20-0.80
Crude fiber: ≤	6.00
Crude ash: ≤	8.00
Methionine + cystine: ≥	0.74

Table 2. Vaccination and prevention protocols

Age (day)	Disease(s)	Route
1	IBD and MD	
5	Coccidiosis	Water
7	ND	Spray
7	IB	Spray
7	IC	Spray
12	Coccidiosis	Water
14	ND	Spray
14	IB	Spray
14	IC	Spray

IBD: Infectious bursal disease, MD: Marek disease, IC: Infectious Coryza

Small intestinal lesion score

Lesions were assessed on a scale ranging from 0 to 4, as follows: 0 = absence of observable lesions, 0.5 = pronounced congestion of serosa and mesentery engorged with blood, 1 = intestines characterized by thin walls and friability with small red petechiae, 2 = localized necrotic lesions, 3 = areas presenting patches of necrosis, and 4 = widespread necrosis.

Sample collection and treatment

On the morning of day 24, every chicken's unique body weight (measured in grams) was recorded. And 2 mL blood samples were collected from the jugular or wing vein. The serum was separated from the clotted whole blood by centrifugation at 3000 g for 10 minutes within 2 hours of collection and stored at -80°C until further analysis. For histological examination, 2.0 cm segments from the duodenum, jejunum, and ileum were fixed in a 4% paraformaldehyde solution for 24 hours. Standard procedures were then followed for paraffin embedding, sectioning to approximately 4 µm, and staining using hematoxylin and eosin. Samples of the duodenal, jejunal, and ileal mucosa, and intestinal contents from the cecum, were collected and promptly frozen in liquid nitrogen at -196°C.

Morphological observation of the small intestine

Imaging of small intestinal tissue sections was performed utilizing a Nikon 80i light microscope (Nikon Corporation, Tokyo, Japan). For each experimental group, small intestinal tissue sections from five chickens were selected. The height of the villi (VL) and the depth of the crypts (CD) were assessed by measuring five villi in each section. Following these measurements, the ratio of villus height to crypt depth (VL/CD) was determined.

Analysis of cecal flora

The sample from the cecal contents was subjected to 16S rRNA sequencing at Majorbio Bio-Pharm Technology Co. Ltd. in Shanghai, China. Bioinformatics analysis was conducted utilizing the Majorbio Cloud Platform (He *et al.*, 2021). Alpha diversity analysis was carried out using Mothur software (version 1.30.2). Beta diversity was assessed through Bray-Curtis principal coordinates analysis (PCoA), and the significance of bacterial segregation among groups was determined by ANOSIM analysis. Linear Discriminant Analysis (LDA) effect size (LEfSe) was used to examine differences in the gut microbiota composition between different groups (Zhao *et al.*, 2024). PICRUST analysis was executed to anticipate the potential functions of the microbiota (Langille *et al.*, 2013).

Analysis of serum metabolomics

The serum samples were analyzed using LC-MS/MS at Majorbio Bio-Pharm Technology Co. Ltd. in Shanghai, China. Multivariate statistical analysis was conducted

using the ropls (Version 1.6.2) R package from Bioconductor on the Majorbio Cloud Platform. Principle component analysis (PCA) was conducted using an unsupervised approach to provide an overview of the metabolic data, and visualize general clustering, trends, or outliers (Ringnér, 2008). Orthogonal partial least squares discriminant analysis (OPLS-DA) was employed for statistical analysis to discern global metabolic alterations among comparable groups (Gennebäck *et al.*, 2013). Model validity was assessed based on model parameters R² and Q², which offer insights into the interpretability and predictability of the model, thereby reducing the possibility of overfitting. Variable importance in the projection (VIP) was calculated in the OPLS-DA model. p-values were estimated using paired Student's t-test in single-dimensional statistical analysis. VIP values larger than 1 and p-values less than 0.05 were used to identify statistically significant differences between the groups. By employing metabolic enrichment and database search for pathway analysis, the different metabolites between the two groups were compiled and mapped to their corresponding biochemical pathways.

Quantitative Real-Time PCR

Total RNA was extracted from the jejunal mucosa with the Trizol reagent provided by Nanjing Vazyme Biotech Co., Ltd., China. The amount and purity of RNA were assessed by measuring absorbance at 260 nm and 280 nm. For reverse transcription, 1 µg of the extracted RNA was processed using the HiScript II RT SuperMix for qPCR, which comes with a gDNA wiper from Nanjing Vazyme Biotech Co., Ltd., China. Quantitative Real-time PCR was performed following the manufacturer's guidelines, using the 2×SYBR Green PCR Mix from Aidlab Biotechnologies Co., Ltd., China. Each sample was measured in triplicate. The relative quantification of gene expressions was calculated using the 2^{-ΔΔCt} method, with 18S rRNA serving as the internal reference gene (Burge *et al.*, 2012). The primer sequences were synthesized by Sangon Biotech Co., Ltd, located in Shanghai, China. The specific information about these primers is presented in Table 3.

Western blot

Jejunal mucosa protein was extracted from the protein lysate, and its concentration was measured using the bicinchoninic acid (BCA) protein assay kit (Beyotime, Shanghai, China). The Western blotting procedure followed the methodology described in previous studies (Lirong *et al.*, 2019). Briefly, proteins were separated by SDS-PAGE and transferred onto a polyvinylidene difluoride (PVDF) membrane. The membrane was then blocked with 5% skimmed milk for 2 hours before being incubated overnight at 4°C with primary antibodies. Secondary antibodies conjugated with horseradish peroxidase were applied at room temperature for 1 hour (AS014, ABclonal Technology, Wuhan, China). Protein

detection was performed using an ECL substrate, and the bands were visualized through electrochemical luminescence (ECL). The primary antibodies used included rabbit anti-Raf1 (A19638), rabbit anti-ERK1/2 (A16686), rabbit anti-p-ERK1/2 (AP0485), rabbit anti-MEK1/2 (A4868), rabbit anti-p-MEK1/2 (AP0209), and β -actin (AC026), all purchased from ABclonal Technology, Wuhan, China.

Immunohistochemistry

The distribution and expression of proteins in the jejunum were observed following the immunohistochemical staining procedures outlined in

previous studies (Zhang et al., 2022a). PCNA (Proliferating Cell Nuclear Antigen) was procured from Gene Tech (Shanghai) Company Limited (GM087902, Gene Tech, Shanghai).

Statistical analysis

The data were analyzed using one-way ANOVA and Dunnett's multiple comparison test employing GraphPad Prism 7.0 software. Correlation analysis was performed using SPSS Statistics 27 (SPSS, Inc., Chicago, USA). The data are presented as means \pm SD. A significance level of $p < 0.05$ indicates a significant difference.

Table 3. Primers used for quantitative real-time PCR

Gene	Primer sequence (5'-3')	Product size/bp	Accession Number	Reference
<i>18S</i>	F:CTCTTCTCGATTCCGTGGGT R:CATGCCAGAGTCTCGTTTCGT	96	XM_417846.8	(Simon et al., 2018)
<i>Occludin</i>	F: GCAGATGTCCAGCGTTACT R: GCAGAGCAGGATGACGATGA	160	NM_205128.1	
<i>Claudin-1</i>	F: GTGTTTCAGAGGCATCAGGTATC R: GTCAGGTCAAACAGAGGTACAA	107	NM_001013611.2	
<i>Claudin-2</i>	F: CTTTGCTTCATCCCACTGGT R: TCAAATTTGGTGCTGTCAGG	86	NM_001277622.1	(Xie, 2019)
<i>ZO-1</i>	F: GGAGTACGAGCAGTCAACATAC R: GAGGCGCACGATCTTCATAA	101	XM_413773	(Emami et al., 2019)
<i>ZO-2</i>	F: GCGTCCCATCCTGAGAAATAC R: CTTGTTCACCTCCCTTCCTCTC	89	NM_204918	(Emami et al., 2019)
<i>MUC2</i>	F: ACCAAGCAGAAAAGCTGGAA R: AAATGGGCCCCTCTGAGTTTT	101	NM_001318434.1	(Xie, 2019)
<i>Raf1</i>	F: GCGAAATGGGATGACCTT R: TGTGTAGTGAGCGGAACG	201	XM_040646131.2	(Zhang et al., 2022b)
<i>ERK</i>	F: ACCTCAGCAACGACCACATT R: GAGCCAGTCCGAAGTCACAA	156	NM_204150.2	
<i>MEK</i>	F: GCAGGGCACCCATTACTC R: AGGTCGGCTGTCCATTCC	226	NM_205388.2	
<i>PCNA</i>	F: GCAGATGTTCTCTCGTTGTGGAG R: GAGCCTTCCTGCTGGTCTTCAATC	95	NM_204170.2	(Xu et al., 2020)

PCNA: Proliferating Cell Nuclear Antigen is a nuclear protein that plays a crucial role in DNA replication, repair, and cell cycle regulation

RESULTS

Body weight and small intestinal lesion score

The body weight of chickens in the NE group was significantly reduced when compared to the CON and F groups (Figure 2A, $p < 0.05$). No significant difference in small intestinal lesion scores was observed between the F and CON groups (Figure 2B, $p > 0.05$), but the lesion score in the NE group was considerably higher than those in the CON and F groups (Figure 2B, $p < 0.05$).

Intestinal histopathology

In both the CON and F groups, the duodenum, jejunum, and ileum had maintained their structural integrity; no obvious pathological changes had been observed (Figure 3A-F). The villi structure of the duodenal intestine in the NE group exhibited clarity, and no evident histopathological alterations were discerned (Figure 3G).

The jejunal intestinal epithelial cells displayed pronounced necrosis and shedding (Figure 3H, arrow), while the ileal villi exhibited atrophy, appearing shortened and thickened (Figure 3I, arrow).

Intestinal villus length and crypt depth

In the duodenum, compared with the CON group, the length of intestinal villi (VL) in both the F and NE groups had exhibited no statistically significant changes ($p > 0.05$), albeit with a marginal decrease in crypt depth (CD) and a slight increase in VL/CD (Figure 4). Moving to the jejunum, compared to the CON group, the variations in VL, CD, and VL/CD within the F group had been no significant difference ($p > 0.05$); whereas in comparison to the CON group, both VL and VL/CD in the NE group had demonstrated a reduction, albeit without a significant

statistical significance ($p > 0.05$). Lastly, examining the ileum, in comparison to the CON group, both VL and VL/CD had exhibited a significant increase in the F group ($p < 0.05$); whereas VL/CD in the NE group, while lower than that of the CON group, had been markedly inferior to that of the F group ($p < 0.05$).

Relative mRNA expression of tight-junction protein and mucin in the jejunum of chickens

Compared to the CON group, the F group showed a significant upregulation of *OCN* and *CLDN1* expression (Figure 5, $p < 0.05$), while *CLDN2* levels were significantly reduced ($p < 0.05$). Although *ZO1*, *ZO2*, and *MUC2* expression levels increased, the changes were not statistically significant ($p > 0.05$). In contrast, the NE group exhibited a non-significant decline in *OCN*, *ZO2*, and *MUC2* expression ($p > 0.05$), whereas *CLDN1*, *CLDN2*, and *ZO1* levels were significantly lower than in the CON group ($p < 0.05$). Additionally, *OCN*, *CLDN1*, *ZO1*, and *ZO2* expression in the NE group was markedly reduced compared to the F group ($p < 0.05$), while *MUC2* levels declined without statistical significance. These findings clearly suggest that the intestinal epithelial barrier integrity was compromised in the NE group.

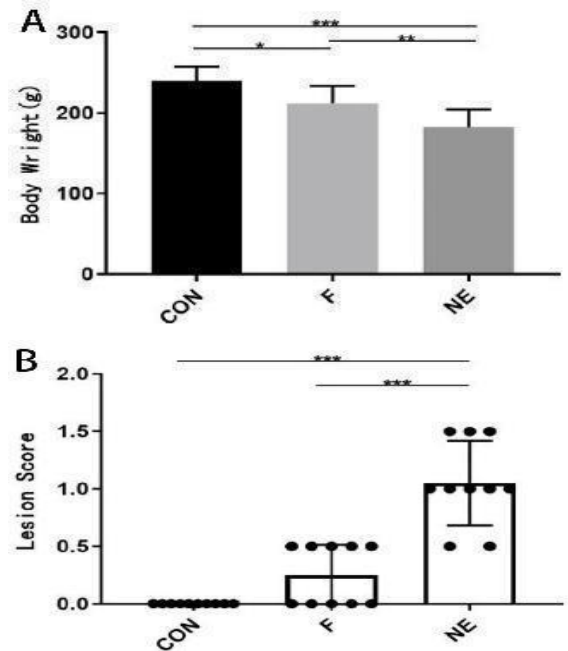


Figure 2. Body weight and small intestinal lesion score of 24-day-old chickens in each group. **A:** Body Weight; **B:** Lesion Score. CON: Negative control group; F: Fishmeal-supplemented diet group; NE: Necrotic Enteritis-induced group (*C. perfringens* challenge). Data are presented as means \pm SD. * $P < 0.05$, ** $P < 0.01$, *** $P < 0.001$.

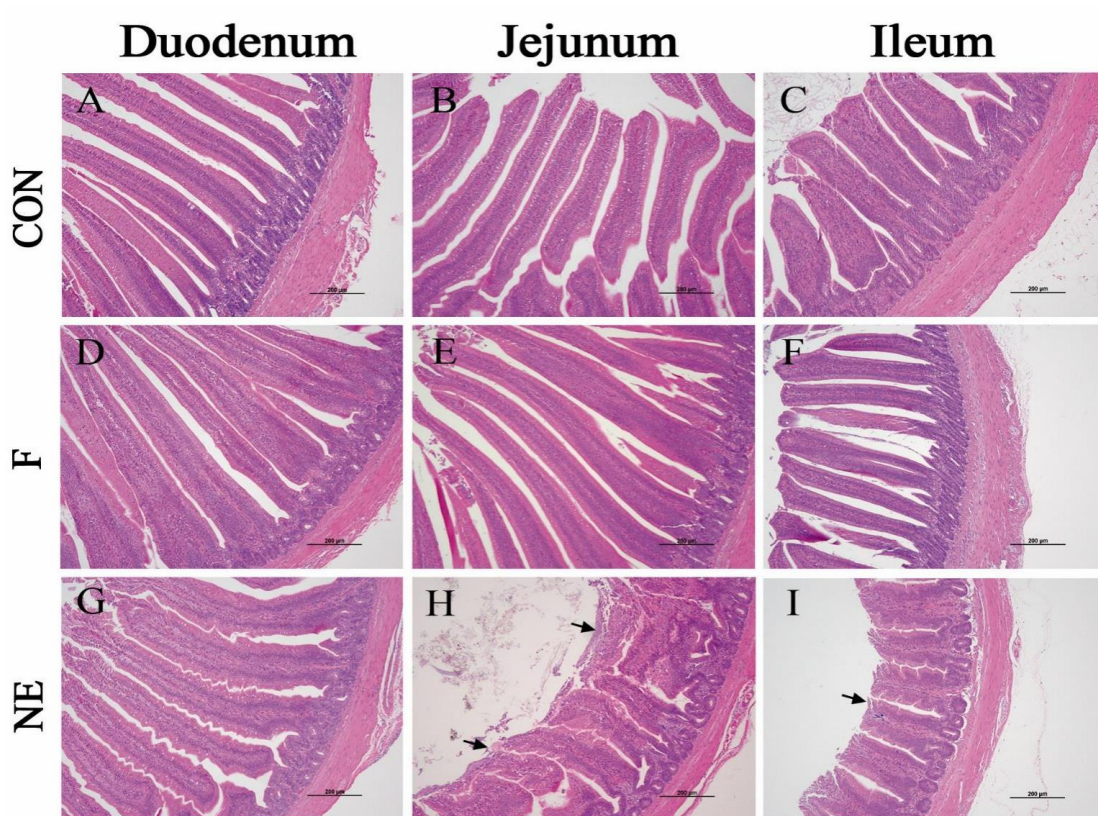


Figure 3. Histopathological observation of small intestine in 24-day-old chickens. CON: Negative control group; F: Fishmeal-supplemented diet group; NE: Necrotic Enteritis-induced group (*C. perfringens* challenge). Scale bars = 200 μ m. **A, D, G:** Duodenum; **B, E, H:** Jejunum; **C, F, I:** Ileum.

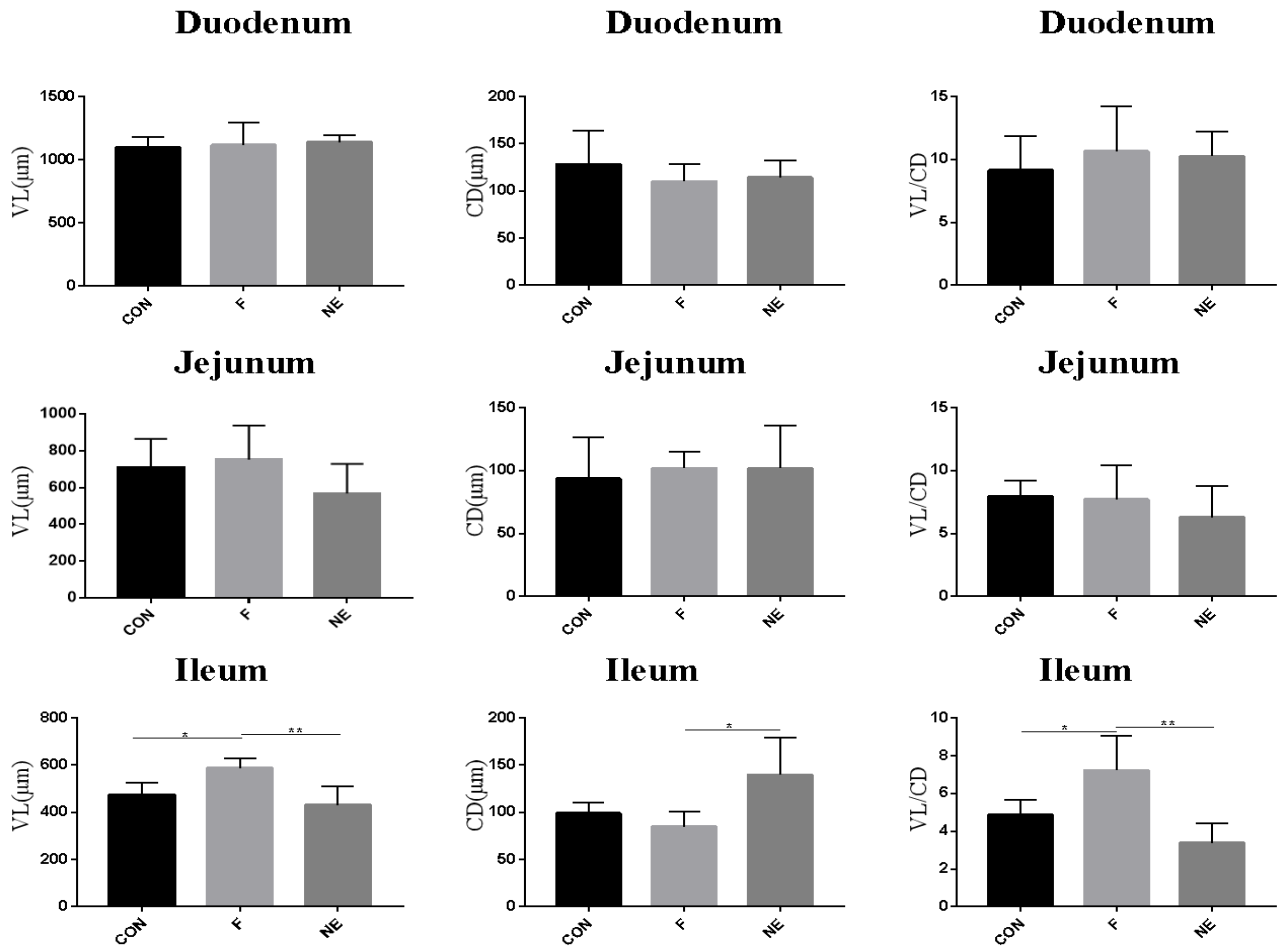


Figure 4. Length of intestinal villus and crypt depth of chickens in each group. CON: Negative control group; F: Fishmeal-supplemented diet group; NE: Necrotic Enteritis-induced group (*C. perfringens* challenge). Data are presented as means \pm SD. * $P < 0.05$, ** $P < 0.01$.

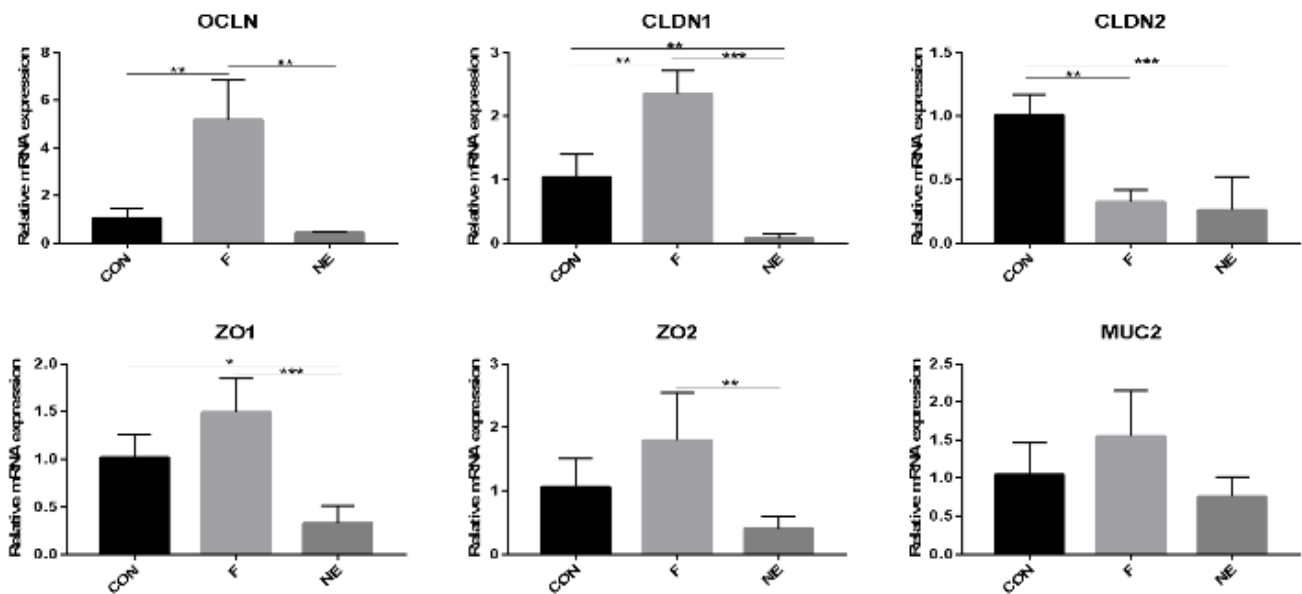


Figure 5. Expression of intestinal tight junction proteins and mucin genes in chickens of all groups. OCLN: Occludin; CLDN1: Claudin-1; CLDN2: Claudin-2; ZO1: Zonula occludins -1; ZO2: Zonula occludins-2; MUC2: Mucin2. CON: Negative control group; F: Fishmeal-supplemented diet group; NE: Necrotic Enteritis-induced group (*C. perfringens* challenge). Data are presented as means \pm SD (n=3). * $P < 0.05$, ** $P < 0.01$, *** $P < 0.001$.

Intestinal flora diversity

The Chao and Shannon indices served as metrics for assessing α diversity, including the richness and diversity of the gut microbiota (Haegeman et al., 2013). The analysis indicated that microbial diversity in the NE group was significantly lower than in both the CON and F groups (Figures 6A, B). To assess β diversity, which

reflects variations in gut bacterial composition, Principal Coordinate Analysis (PCoA) was conducted. The microbial community structure in the F group exhibited significant differences compared to the CON and NE groups ($p < 0.05$). However, the NE group's microbiota composition closely resembled that of the CON group (Figure 6C).

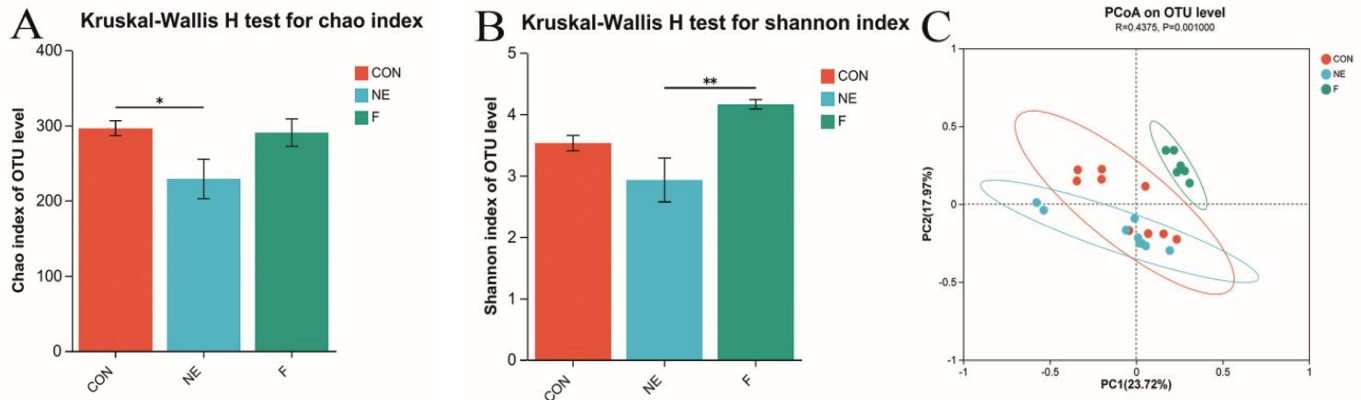


Figure 6. Diversity and structure of intestinal flora. **A:** Chao index; **B:** Shannon index; **C:** PCoA analysis of intestinal flora based on Bray-Curtis distance. CON: Negative control group; F: Fishmeal-supplemented diet group; NE: Necrotic Enteritis-induced group (*C. perfringens* challenge)

Linear discriminant analysis effect size (LEfSe) analysis of intestinal flora

Linear discriminant analysis (LDA) effect size (LEfSe) analysis was used to detect significant differences in intestinal flora among the three groups at both the family and genus levels. The results revealed distinct taxa enrichment across the three groups. In group CON, taxa such as *Lactobacillus*, *norank_f_Ruminococcaceae*, *Blautia*, and *Ruminococcus gauvreauii* group were significantly enriched. In contrast, group NE exhibited a marked increase in *f_Clostridiaceae*, *Subdoligranulum*, *Erysipelatoclostridium*, *Anaerofilum*, and *Candidatus Arthromitus*. Meanwhile, group F showed notable enrichment in *norank_f_norank_o_Clostridia* UCG-014, *Negativibacillus*, *norank_f_norank_o_Clostridia* vadinBB60 group, *Colidextribacter*, *norank_f_Clostridium methylpentosum* group, and *Escherichia-Shigella* (Figure 7).

Analysis of PICRUSt

PICRUSt was employed to predict the gene functions of the cecal microbiota of chicks in the CON, NE, and F groups. The results showed a strong correlation between the intestinal microbiota and microbial metabolism in diverse environments (Figure 8).

Serum metabolomics

Serum metabolites were detected using the LC-MS/MS method. PCA analysis revealed significant differences ($p < 0.05$) in serum metabolites among all groups (Figure 9A, B). Furthermore, OPLS-DA analysis revealed significant differences ($p < 0.05$) in serum metabolites among all groups (Figure 9C-F).

Perform KEGG enrichment analysis and screen the differential metabolic pathways between group F and group CON, as well as between group NE and group CON. The outcomes demonstrated 14 distinct metabolic pathways between group F and group CON (Figure 10A), mainly centered on Arginine biosynthesis, Purine metabolism, and Glycerophospholipid metabolism. Fourteen distinct metabolic pathways were identified between the NE group and the CON group (Figure 10B), primarily focused on signal transduction pathways such as MAPK, VEGF, and ErbB signaling pathways. The findings indicated that differential metabolic pathways in group F primarily centered around metabolic pathways associated with amino acid, nucleotide, and lipid metabolism. In contrast, differential metabolic pathways in group NE were primarily focused on metabolic pathways related to cell proliferation, migration, and differentiation, such as the MAPK signaling pathway.

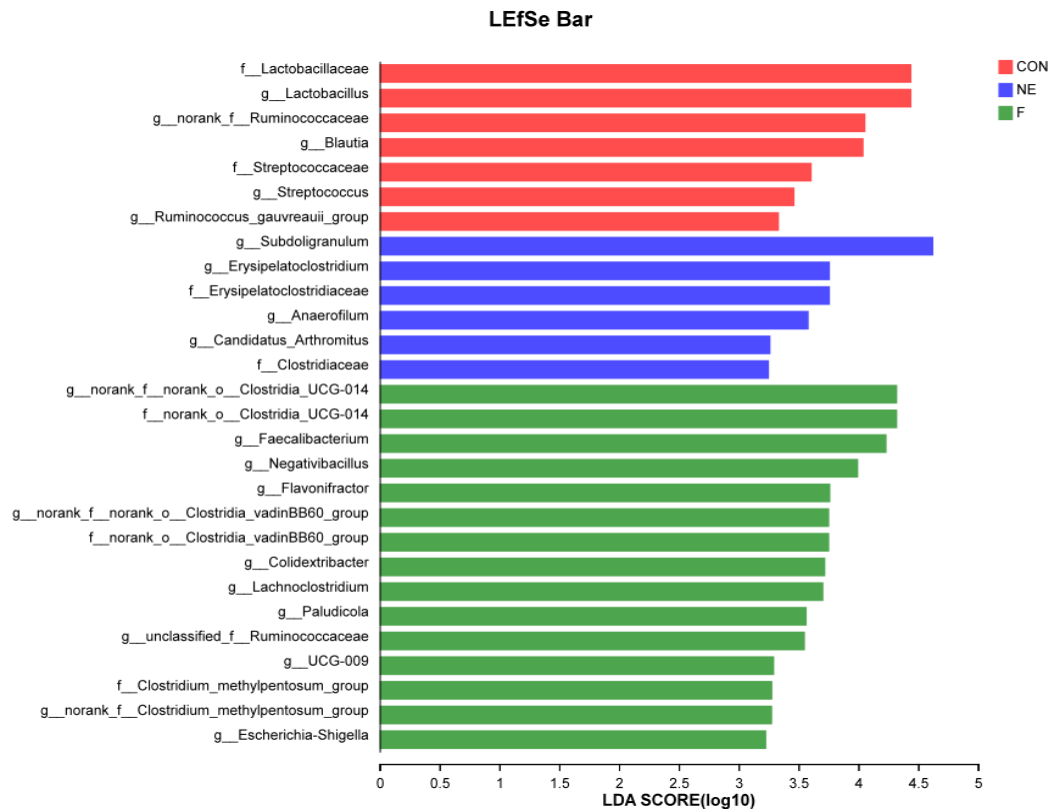


Figure 7. LEfSe analysis of intestinal flora. LDA score>3.2 was considered as the screening condition to obtain differential intestinal flora.

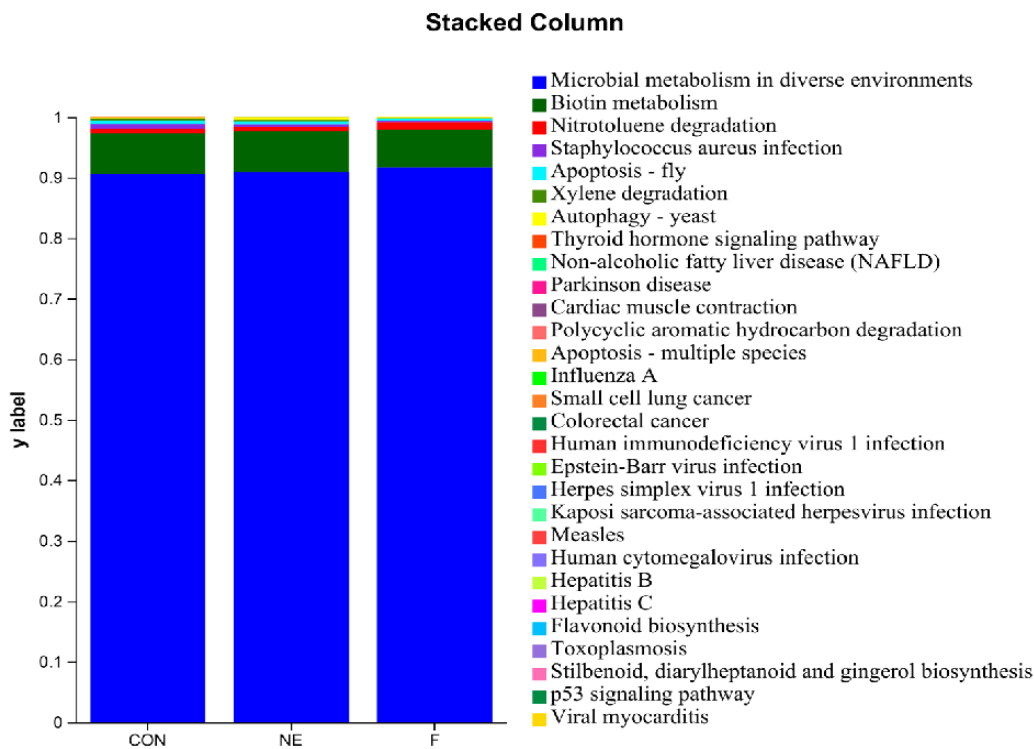


Figure 8. Functional gene prediction of gut microbiota in necrotic enteritis. Histogram Analysis of Metabolic Pathways by Strain (Abscissa: Experimental Groups, Ordinate: Pathway Abundance%) in White Lohmann Chickens.

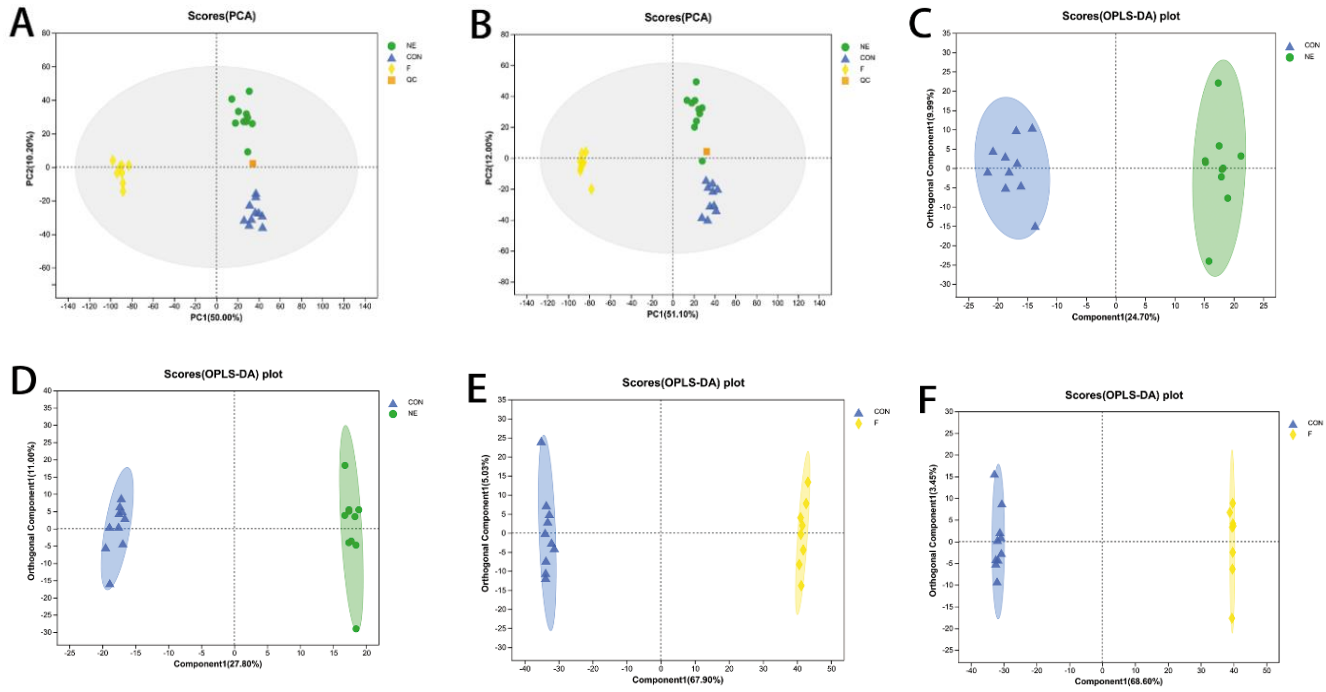


Figure 9. Metabolic profiling in chicken necrotic enteritis: PCA and OPLS-DA Scatter Plots. **A, B:** Principal component analysis (PCA) of chickens. **C-F:** Orthogonal partial least squares discrimination analysis (OPLS-DA) scatter plots of chickens.

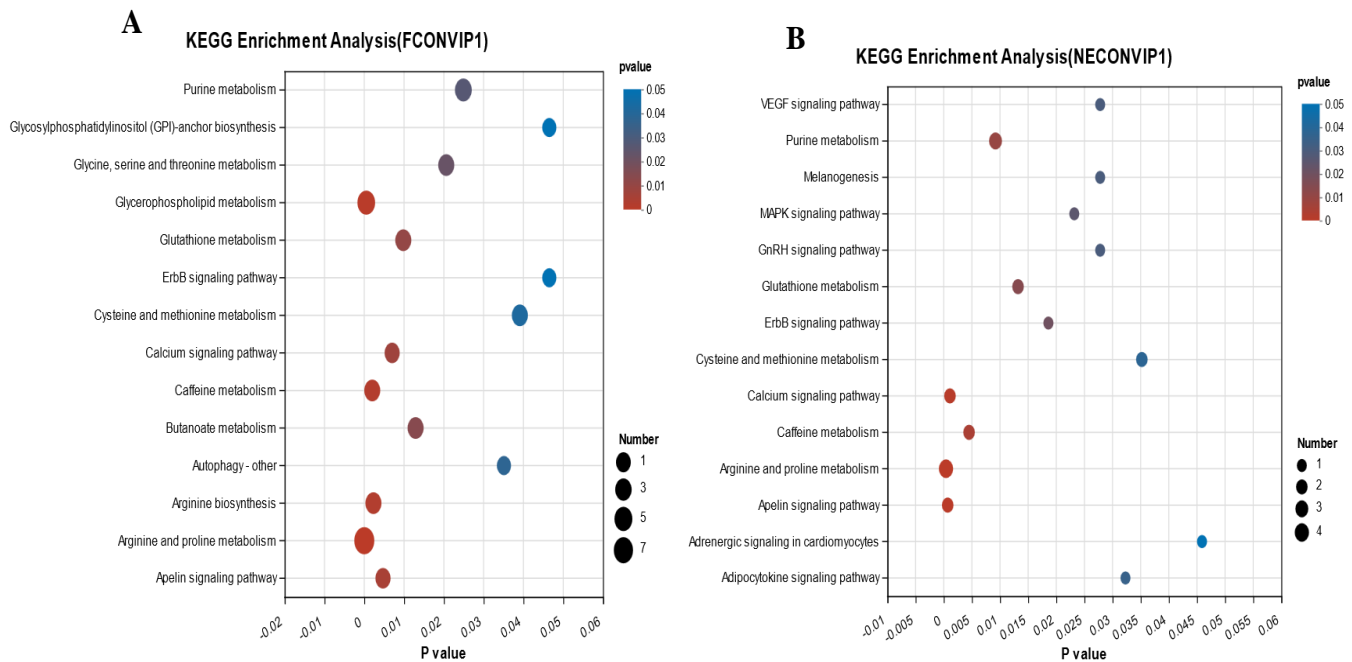


Figure 10. KEGG enrichment analysis reveals functional divergence in metabolic pathways. Amino Acid/Nucleotide Metabolism in Group F versus Cell Proliferation Signaling in Group NE (F/CON: n = 14 pathways; NE/CON: n = 14 pathways), **A:** Differential metabolic pathways between group F and group CON, **B:** Differential metabolic pathways between group NE and group CON. A p-value less than 0.05 was considered the screening condition to obtain differential metabolic pathways.

Intestinal flora and serum metabolomics

To elucidate the potential functional interplay between intestinal microbiota and serum metabolomics. An association analysis was conducted on the top 20 microbiota and metabolites exhibiting intergroup differences. In the F and CON groups, 10 metabolites were identified that demonstrated significant positive correlations with *g__Lactobacillus* and substantial negative correlations with *g__Negativibacillus*. These metabolites include diacylglycerols such as DG (18:0/18:2(9Z,12Z)/0:0), DG (18:2(9Z,12Z)/18:1(9Z)/0:0),

DG (20:1(11Z)/18:4(6Z,9Z,12Z,13Z)/0:0) (Figure 11A). In both the NE and CON groups, four metabolites were observed to show negative correlations with *g__Anaerotruncus*, namely Malic acid, D-(+)-Malic acid, Xanthine and Xanthosine. Moreover, Malic acid and D-(+)-Malic acid displayed significant positive associations with *g__Erysipelatoclostridium*, *g__Lachnospiraceae_NK4A136_group*, and *g__Subdoligranulum*, while showing marked negative correlations with *g__Fournierella* (Figure 11B).

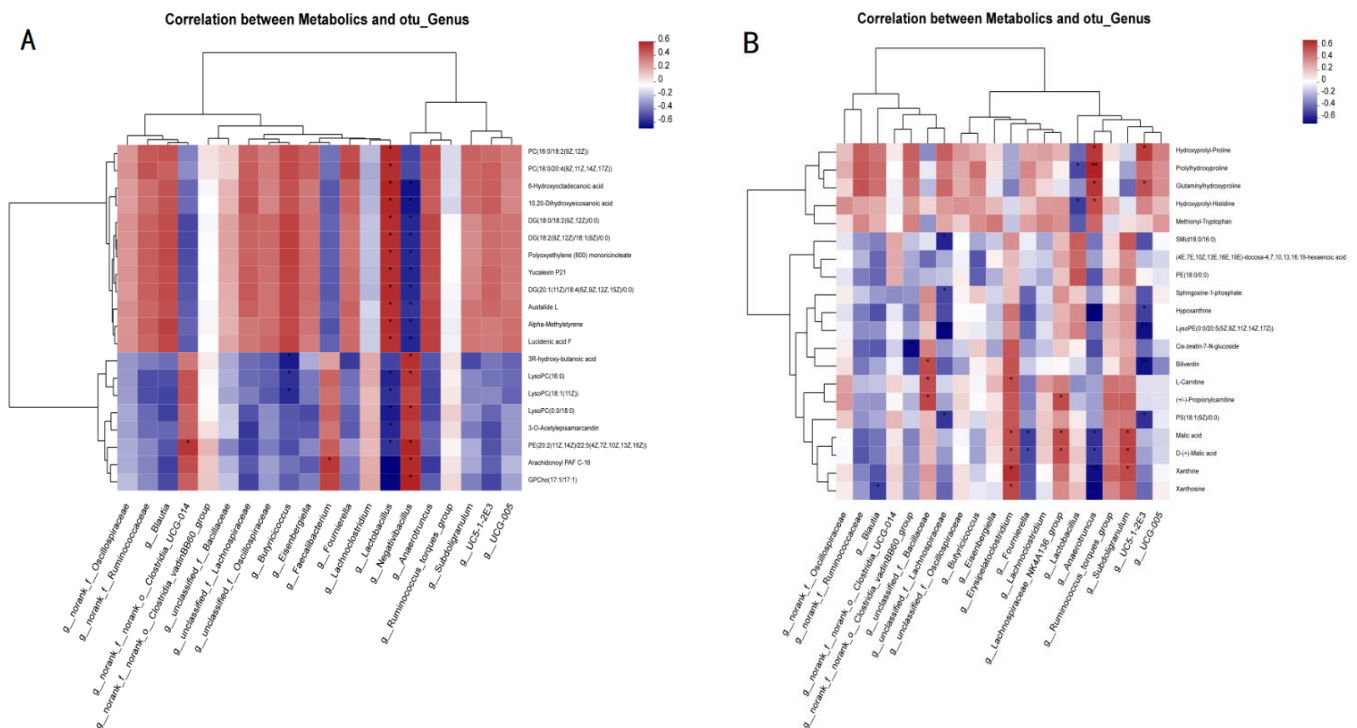


Figure 11. Integrated correlation analysis of gut microbiota and serum metabolites in 24-Day-Old white leghorn chickens with necrotic enteritis. A: Correlation analysis of intestinal flora and serum metabolites between group F and group CON; B: Correlation analysis of intestinal flora and serum metabolites between group NE and group CON. Red means positive correlation, and blue means negative correlation. Data are presented as means \pm SD. * $P < 0.05$, ** $P < 0.01$.

Expression of MAPK/ERK signaling pathway related genes in jejunum

The relative mRNA expression levels of *Raf1*, *ERK*, and *MEK* in the MAPK/ERK signaling pathway were measured using real-time fluorescence quantitative PCR. As shown in Figure 12, compared to the CON group, the mRNA expression levels of *Raf1*, *ERK*, and *MEK* were significantly increased in the F group ($p < 0.05$). In contrast, the NE group exhibited a decrease in *Raf1* mRNA expression ($P > 0.05$) and a significant reduction in *ERK* and *MEK* mRNA levels ($p < 0.05$) compared to the CON group. Furthermore, when compared to the F group, the mRNA expression levels of *Raf1*, *ERK*, and *MEK* in the NE group were significantly lower ($p < 0.05$). These

results indicate that the MAPK/ERK pathway is suppressed in the NE group.

Expression of proliferating cell nuclear antigen PCNA in the jejunum

The expression of the PCNA gene in the jejunum was assessed using qPCR and immunohistochemistry (IHC). As illustrated in Figure 13, compared to the CON group, chickens in the F group exhibited an elevated PCNA expression level in the jejunal mucosa, although this difference lacked statistical significance ($p > 0.05$). In contrast, the NE group demonstrated a marked reduction in PCNA immunostaining intensity compared to both the F and CON groups, with this decrease reaching statistical significance ($p < 0.05$).

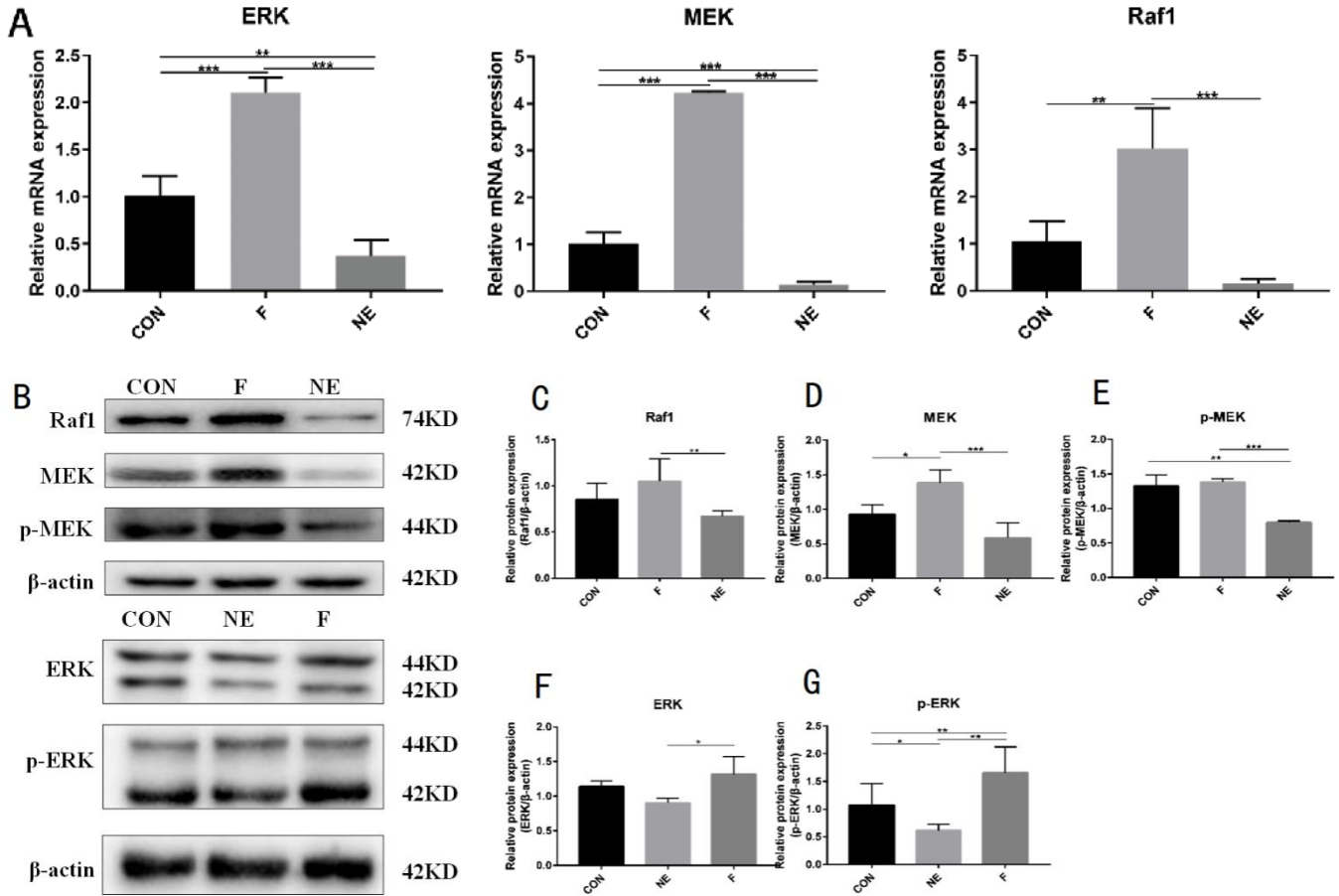


Figure 12. Expression of genes related to the MAPK/ERK signaling pathway. **A:** The relative mRNA expression of MAPK/ERK signaling pathway-related genes. **B:** Protein levels of MAPK/ERK signaling pathway-related genes. **C-G:** Results of the gray-scale analysis of the corresponding protein bands. β -actin served as the loading control. CON: Negative control group; F: Fishmeal-supplemented diet group; NE: Necrotic Enteritis-induced group (*C. perfringens* challenge). Data are presented as means \pm SD. * $P < 0.05$, ** $P < 0.01$, *** $P < 0.001$.

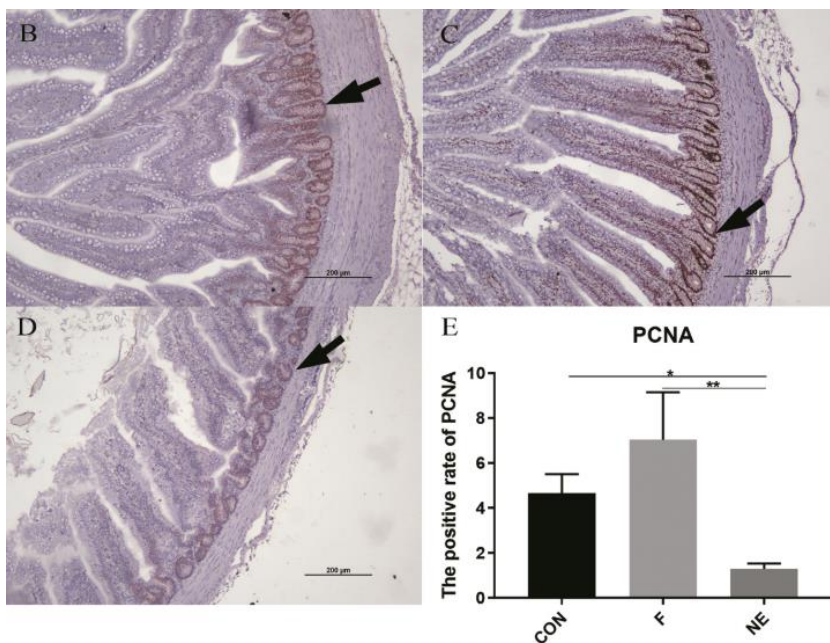


Figure 13. Expression of proliferating cell nuclear antigen (PCNA) gene in jejunum tissue of chickens. **A:** Relative mRNA expression of the PCNA gene. **B-C:** The protein distribution and expression levels of PCNA in the jejunum (IHC, 100 \times). PCNA positive staining shows a brown signal. **E:** Statistical analysis of PCNA positive rate. CON: Negative control group; F: Fishmeal-supplemented diet group; NE: Necrotic Enteritis-induced group (*C. perfringens* challenge). Scale bars = 200 μ m. Data are presented as means \pm SD. * $P < 0.05$, ** $P < 0.01$.

DISCUSSION

Chicken necrotic enteritis stands as a recurrent enteric malady within the poultry sector, imposing an annual financial burden of approximately 600 million on the global poultry industry (Wade et al., 2015). The mere presence of *C. perfringens* is insufficient to instigate necrotic enteritis; prevalent modeling approaches encompass co-induction scenarios involving coccidia/*C. perfringens* or fishmeal/*C. perfringens* (Huang et al., 2018; Keerqin et al., 2021). Coccidiosis has the potential to inflict harm upon the intestinal mucosa, prompting the host to generate copious amounts of mucus, thereby fostering a conducive environment for the rapid colonization and multiplication of bacteria (Collier et al., 2008). Supplementation of the diet with high animal protein content (fishmeal) will escalate the reproductive rate of *C. perfringens* within the intestine, consequently leading to damage to the intestinal epithelium by the bacteria and their toxins (NetB toxin, alpha toxin and beta toxin) (Keerqin et al., 2021). Given that coccidia infection can induce substantial intestinal damage in chickens (Adhikari et al., 2020), making it indistinguishable from necrotic enteritis, the current study opted for high animal protein fish meal as the inducing agent (Drew et al., 2004b; Williams, 2005; Kaldhusdal et al., 2016).

Necrotic enteritis in chickens predominantly targets the small intestine, with the jejunal and ileal regions exhibiting the highest susceptibility to pathological damage (Goossens et al., 2020). The disease typically presents in a subclinical manner, characterized by minimal chicken mortality, yet causing intestinal damage resulting in compromised nutrient absorption and subsequent weight loss (Timbermont et al., 2011; Caly et al., 2015; Lee and Lillehoj, 2022). Throughout this study, there were no instances of mortality among the chickens in any experimental group. Relative to the other two groups, the body weight of chickens in the infected group exhibited a notable decrease, concomitant with significant small intestinal lesions. Within the infection group, the jejunum displayed shedding and necrosis of intestinal epithelial cells, while the ileum exhibited shortened villi. The integrity of the intestinal epithelial barrier is influenced by various factors, with intestinal tight junction proteins and mucus playing pivotal roles in preventing pathogen infiltration through the epithelial barrier. During the onset of chicken necrotic enteritis, *C. perfringens* generates a toxin that interferes with the tight junctions among intestinal epithelial cells, resulting in decreased expression

of tight junction proteins such as Occludin, Claudin-1, and ZO-1, as well as mucin MUC2 in the chicken intestine (Gharib-Naseri et al., 2020; Park et al., 2022). Following necrotic enteritis progression, the infected group showed decreased expression of intestinal barrier-associated proteins, specifically Claudin-1, Occludin, ZO-1, ZO-2, and the mucin MUC2.

It has been reported that the inclusion of fish meal or a combination of fish meal and *C. perfringens* in the diet can lead to substantial alterations in the intestinal flora of chickens, thereby indirectly providing insights into the health status of poultry by examining the intestinal flora composition (Stanley et al., 2014). In the current study, high-throughput sequencing technology was used to analyze the cecal microbiota of chickens. The results showed a decrease in species diversity in the ceca of chickens fed a high fishmeal diet, with a notable reduction in beneficial bacterial genera such as *Faecalibacterium* and *Oscillospira*, and an increase in potentially harmful bacterial groups such as *Escherichia* and *Enterobacteriaceae*. These findings are consistent with previous studies on necrotic enteritis in chickens, indicating a disruption in the balance of the gut microbiota that may negatively impact intestinal health. *Lactobacillus*, a crucial probiotic residing in the intestines of humans and animals, is vital for enhancing the immune function of the intestinal mucosa, inhibiting intestinal inflammation, and curbing the growth of both intestinal pathogens and foodborne pathogens (Xu et al., 2018). *C. perfringens* infection results in a decreased relative abundance of *Lactobacillus*, *Blautia*, and *Ruminococcus*. Notably, *Ruminococcaceae* and *Blautia* are producers of short-chain fatty acids, crucial for providing energy to the intestinal epithelium and preserving epithelial integrity (Wang et al., 2021b; Koh et al., 2016; Bortoluzzi et al., 2019). In chickens suffering from necrotic enteritis, the relative abundance of *Erysipelothrixaceae* and *Clostridium* significantly increased. Notably, the abundance of *Erysipelothrixaceae* exhibited a negative correlation with body fat weight, colonic butyrate concentration, and overall intestinal health (Pham et al., 2020). In the present study, the abundance of *g_Lactobacillus*, *g_Blautia*, and *g_Ruminococcus_gauvreui_group* decreased in both the F and NE groups, while the abundance of *g_norank_f_norank_o_Clostridia_UCG-014*, *g_norank_f_norank_o_Clostridia_vadinBB60_group*, *g_Colidextribacter*, and *g_Escherichia-Shigella* increased in the F group, and the abundance of *f_Clostridiaceae* and *g_Erysipelatoclostridium*

increased in the NE group. These findings indicated that fish meal has the potential to alter the intestinal environment and disrupt the balance of intestinal flora, thereby promoting the growth and colonization of intestinal pathogens. Moreover, when fish meal is combined with *C. perfringens*, it leads to a superimposition of the intestinal flora composition in chickens with necrotic enteritis, causing a marked reduction in beneficial intestinal flora and a notable increase in harmful flora (Wu *et al.*, 2014).

By conducting an enrichment analysis of differential metabolic pathways associated with distinct metabolites, it was discovered that the fishmeal group predominantly engaged in amino acid metabolism, including arginine and proline metabolism, nucleotide metabolisms like purine metabolism, lipid metabolism such as glycerophospholipid metabolism, and other various metabolic pathways. Furthermore, the differential metabolic pathway in the infection group primarily centered on the MAPK signaling pathway, which is closely associated with cell proliferation, differentiation, and migration. Analysis of gut microbiota gene function predictions revealed that the majority of microbiota alterations were linked to metabolism, suggesting the existence of substantial differences in metabolic function across treatments. An examination of the correlation between serum differential metabolites and intestinal flora among the groups revealed significant associations between *g__Lactobacillus* and *g__Negativibacillus* with the metabolite diglyceride (DG). DG, in turn, is implicated in various signaling pathways such as the MAPK, VEGF, and ErbB pathways, all of which play critical roles in regulating cell proliferation, differentiation, and migration (Din *et al.*, 2025). Additionally, metabolites such as malic acid, D-Malic acid, and xanthine exhibited significant correlations with *g__Anaerotruncus*, *g__Erysipelatoclostridium*, *g__Lachnospiraceae_NK4A136_group*, *g__Subdoligranulum*, and *g__Fournierella*. Malic acid is intricately associated with the tricarboxylic acid cycle (TCA cycle), a pivotal component of the body's energy metabolism (MacCannell and Roberts, 2022). D-malic acid is intricately linked to the metabolism of butyrate. The energy sustenance of intestinal epithelial cells predominantly stems from butyrate, a factor pivotal for preserving the integrity of the intestinal barrier (Wang *et al.*, 2021c). Xanthines actively participate in purine metabolism. The intestinal mucosa necessitates heightened concentrations of nucleotides to fuel processes such as energy production, cellular proliferation, and innate

immunity. This demand for nucleotide substrates escalates markedly in response to events like tissue injury, infection, and wound healing, as these processes require extensive cell proliferation (necessitating DNA synthesis), heightened ATP production for energy-intensive repair mechanisms, immune cell activation and expansion to combat pathogens, and synthesis of structural proteins such as mucins to restore epithelial barrier integrity (Lee *et al.*, 2020). The aforementioned observations illuminate that these microbial communities may be intricately engaged, either directly or indirectly, in the biosynthesis of these metabolites. Furthermore, these metabolites bear relevance to essential cellular processes encompassing survival, proliferation, and differentiation.

ERK (Extracellular Signal-Regulated Kinase), situated within the cytoplasm, belongs to the MAPK family. Following activation, it translocate to the nucleus, orchestrating the modulation of various transcription factors through phosphorylation. Moreover, it instigates gene expression in response to extracellular stimuli, playing a pivotal role in cellular processes such as proliferation, migration, differentiation, and apoptosis (Guo *et al.*, 2020). Investigations revealed the inhibition of the ERK signaling pathway following intestinal injury. Some studies have also suggested that the ERK signaling pathway is involved in the proliferation and differentiation of epithelial cells following intestinal mucosal injury, and inhibition of this pathway exacerbates intestinal damage and apoptosis (ZHAN Yuanquan 2022). In the present study, suppression of ERK signaling pathway-related gene expression was observed in infected chickens, indicating impaired proliferation of intestinal epithelial cells in chickens with necrotic enteritis, which hindered post-injury intestinal repair. Notably, the MAPK/ERK signaling pathway intricately influences the expression of tight junction proteins; its inhibition correlates with a diminished expression of the tight junction protein Claudin-1. In both *in vivo* and *in vitro* experiments, it has been demonstrated that the activation of the ERK signaling pathway has the capability to enhance the expression of intestinal tight junction proteins (Dai *et al.*, 2012). In the present study, it was observed that the expression of tight junction proteins in the intestinal tract of chickens in the infection group exhibited a decline, a phenomenon that could potentially be attributed to the mediation of the ERK signaling pathway. Proliferating cell nuclear antigen (PCNA) is a protein crucial to the cell cycle, predominantly localized in the base and middle regions of intestinal crypts (Y *et al.*, 2016), where it

actively engages in essential DNA metabolism processes, including replication and repair. The synthesis and expression of PCNA are intricately linked to the process of cell proliferation (Morris and Mathews, 1989; Cardano et al., 2020; Wang et al., 2022). The current investigation revealed a significant decrease in PCNA expression among chickens in the infection group in comparison to both the negative control group and the fish meal group, suggesting a hindrance in the proliferation of intestinal epithelial cells in chickens afflicted with necrotic enteritis, consequently leading to impaired renewal and repair mechanisms within the intestinal epithelium.

CONCLUSION

Feeding fish meal alone is insufficient to directly induce necrotic enteritis; however, it exerts a significant impact on the intestinal microbiota composition, leading to a reduction in beneficial flora such as *Lactobacillus* and *Blautia*. The change in the makeup of the intestinal flora encourages the growth of pathogenic *C. perfringens*, which in turn makes it more likely for subclinical necrotic enteritis to develop. Following the onset of necrotic enteritis, the mucosal layers of the jejunum and ileum in afflicted chickens sustain damage, consequently leading to impaired nutrient absorption capabilities. At the same time, an imbalance in the intestinal microbiota, known as dysbiosis, interferes with the MAPK/ERK metabolic pathway. As a result, this hinders the multiplication of intestinal epithelial cells and impairs the restoration of the intestinal epithelial barrier. Further research could focus on exploring potential interventions that can reverse the dysbiosis-induced disruption of the MAPK/ERK metabolic pathway. For example, studying the effects of specific probiotics or prebiotics on modulating the gut microbiota composition and its subsequent impact on the recovery of the intestinal epithelial barrier function through the regulation of the MAPK/ERK pathway. This may lead to the development of novel therapeutic strategies for intestinal diseases related to microbiota imbalance and epithelial barrier dysfunction.

DECLARATION

Funding

This study was financially supported by the National Broiler Industry Technology System No. (CARS-41) and the Hubei Province Agricultural Technology Innovation Center Project under the contract No. (2019-620-000-001-17).

Acknowledgments

The researchers would like to thank the reviewers for their constructive criticisms that helped to improve the quality of this manuscript.

Authors' contributions

Yunting CHU implemented the research and contributed to data collection, database creation, and preparation of the manuscript. Liyue SUN and Yanyi LI were also involved in preparing the manuscript and data analysis. Changqin GU guided the research and manuscript preparation. All authors checked and approved the final version of the manuscript for publishing in the present journal.

Ethical considerations

All authors have checked statistical analysis as well as the ethical issues, including plagiarism, consent to publish, misconduct, data fabrication and/or falsification, double publication and/or submission, and redundancy.

Availability of data and materials

The data of the article will be provided by the corresponding author according to reasonable requests.

Competing interests

There is no competing interest in this research.

REFERENCES

- Adhikari P, Kiess A, Adhikari R, and Jha R (2020). An approach to alternative strategies to control avian coccidiosis and necrotic enteritis. *Journal of Applied Poultry Research*, 29(2): 515-534. DOI: <https://www.doi.org/10.1016/j.japr.2019.11.005>
- Bansal M, Fu Y, Alrubaye B, Abraha M, Almansour A, Gupta A, Liyanage R, Wang H, Hargis B, and Sun X (2020). A secondary bile acid from microbiota metabolism attenuates ileitis and bile acid reduction in subclinical necrotic enteritis in chickens. *Journal of Animal Science and Biotechnology*, 11(3): 767-776. DOI: <https://www.doi.org/10.1186/s40104-020-00441-6>
- Bortoluzzi C, Vieira BS, Hofacre C, and Applegate TJ (2019). Effect of different challenge models to induce necrotic enteritis on the growth performance and intestinal microbiota of broiler chickens. *Poultry Science*, 98(7): 2800-2812. DOI: <https://www.11:37doi.org/10.3382/ps/pez084>
- Burge S, Kelly E, Lonsdale D, Mutowo-Muullenet P, McAnulla C, Mitchell A, Sangrador-Vegas A, Yong SY, Mulder N, and Hunter S (2012). Manual GO annotation of predictive protein signatures: The InterPro approach to GO curation. *Database*, 2012: bar068. DOI: <https://www.doi.org/10.1093/database/bar068>
- Caly DL, D'Inca R, Auclair E, and Drider D (2015). Alternatives to antibiotics to prevent necrotic enteritis in broiler chickens: A microbiologist's perspective. *Frontiers in Microbiology*, 6: 1336. DOI: <https://www.doi.org/10.3389/fmicb.2015.01336>
- Cardano M, Tribioli C, and Prosperi E (2020). Targeting strategy to proliferating cell nuclear antigen (PCNA) as an effective strategy to inhibit tumor cell proliferation. *Current Cancer Drug Targets*, 20(4): 240-252. DOI: <https://www.doi.org/10.2174/1568009620666200115162814>

- Collier CT, Hofacre CL, Payne AM, Anderson DB, Kaiser P, Mackie RI, and Gaskins HR (2008). Coccidia-induced mucogenesis promotes the onset of necrotic enteritis by supporting *Clostridium perfringens* growth. *Veterinary Immunology and Immunopathology*, 122(1-2): 104-115. DOI: <https://www.doi.org/10.1016/j.vetimm.2007.10.014>
- Dai C, Zhao DH, and Jiang M (2012). VSL#3 probiotics regulate the intestinal epithelial barrier *in vivo* and *in vitro* via the p38 and ERK signaling pathways. *International Journal of Molecular Medicine*, 29(2): 202-208. DOI: <https://www.doi.org/10.3892/ijmm.2011.839>
- Din ZU, Cui B, Wang C, Zhang X, Mehmood A, Peng F, and Liu Q (2025). Crosstalk between lipid metabolism and EMT: Emerging mechanisms and cancer therapy. *Mol Cell Biochem*, 480(1): 103-118. DOI: <https://www.doi.org/10.1007/s11010-024-04995-1>
- Drew MD, Syed NA, Goldade BG, Laarveld B, and Van Kessel AG (2004). Effects of dietary protein source and level on intestinal populations of *Clostridium perfringens* in broiler chickens. *Poultry Science*, 83(3): 414-420. DOI: <https://www.doi.org/10.1093/ps/83.3.414>
- Eckel J (2021). Intestinal microbiota and host metabolism - A complex relationship. *Acta Physiologica*, 232(1): e13638. DOI: <https://www.doi.org/10.1111/apha.13638>
- Emami NK, Calik A, White MB, Young M, and Dalloul RA (2019). Necrotic enteritis in broiler chickens: The role of tight junctions and mucosal immune responses in alleviating the effect of the disease. *Microorganisms*, 7(8): 231. DOI: <https://www.doi.org/10.3390/microorganisms7080231>
- Gennebäck N, Malm L, Hellman U, Waldenström A, and Mörner S (2013). Using OPLS-DA to find new hypotheses in vast amounts of gene expression data — Studying the progression of cardiac hypertrophy in the heart of aorta ligated rat. *Gene*, 522(1): 27-36. DOI: <https://www.doi.org/https://doi.org/10.1016/j.gene.2013.03.018>
- Gharib-Naseri K, de Paula Dorigam JC, Doranalli K, Kheravii S, Swick RA, Choet M, and Wu SB (2020). Modulations of genes related to gut integrity, apoptosis, and immunity underlie the beneficial effects of *Bacillus amyloliquefaciens* CECT 5940 in broilers fed diets with different protein levels in a necrotic enteritis challenge model. *Journal of Animal Science and Biotechnology*, 11: 104. DOI: <https://www.doi.org/10.1186/s40104-020-00508-4>
- Goossens E, Dierick E, Ducatelle R, and Van Immerseel F (2020). Spotlight on avian pathology: untangling contradictory disease descriptions of necrotic enteritis and necro-haemorrhagic enteritis in broilers. *Avian Pathology*, 49(5): 423-427. DOI: <https://www.doi.org/10.1080/03079457.2020.1747593>
- Guo YJ, Pan WW, Liu SB, Shen ZF, Xu Y, and Hu LL (2020). ERK/MAPK signalling pathway and tumorigenesis. *Experimental and Therapeutic Medicine*, 19(3): 1997-2007. DOI: <https://www.doi.org/10.3892/etm.2020.8454>
- Haegeman B, Hamelin J, Moriarty J, Neal P, Dushoff J, and Weitz JS (2013). Robust estimation of microbial diversity in theory and in practice. *The ISME Journal*, 7(6): 1092-1101. DOI: <https://www.doi.org/10.1038/ismej.2013.10>
- He Q, Zhou W, Chen X, and Zhang Q (2021). Chemical and bacterial composition of *Broussonetia papyrifera* leaves ensiled at two ensiling densities with or without *Lactobacillus plantarum*. *Journal of Cleaner Production*, 329: 129792. DOI: <https://www.doi.org/https://doi.org/10.1016/j.jclepro.2021.129792>
- Huang T, Gao B, Chen WL, Xiang R, Yuan MG, Xu ZH, and Peng XY (2018). Temporal effects of high fishmeal diet on gut microbiota and immune response in *Clostridium perfringens* challenged chickens. *Frontiers in Microbiology*, 9: 2754. DOI: <https://www.doi.org/10.3389/fmicb.2018.02754>
- Kaldhusdal M, Benestad SL, and Lovland A (2016). Epidemiologic aspects of necrotic enteritis in broiler chickens - disease occurrence and production performance. *Avian Pathology*, 45(3): 271-274. DOI: <https://www.doi.org/10.1080/03079457.2016.1163521>
- Keerqin C, Rhayat L, Zhang ZH, Gharib-Naseri K, Kheravii SK, Devillard E, Crowley TM, and Wu SB (2021). Probiotic *Bacillus subtilis* 29,784 improved weight gain and enhanced gut health status of broilers under necrotic enteritis condition. *Poultry Science*, 100(4): 100981. DOI: <https://www.doi.org/10.1016/j.psj.2021.01.004>
- Kidd MT, Maynard CW, and Mullenix GJ (2021). Progress of amino acid nutrition for diet protein reduction in poultry. *Journal of Animal Science and Biotechnology*, 12(1): 1-9. DOI: <https://www.doi.org/10.1186/s40104-021-00568-0>
- Kyoto Encyclopedia of Genes and Genomes (KEGG). KEGG Database. Available at: <https://www.genome.jp/kegg/>
- Koh A, De Vadder F, Kovatcheva-Datchary P, and Backhed F (2016). From dietary fiber to host physiology: short-chain fatty acids as key bacterial metabolites. *Cell*, 165(6): 1332-1345. DOI: <https://www.doi.org/10.1016/j.cell.2016.05.041>
- Langille MGI, Zaneveld J, Caporaso JG, McDonald D, Knights D, Reyes JA, Clemente JC, Burkepille DE, Vega Thurber RL, Knight R et al. (2013). Predictive functional profiling of microbial communities using 16S rRNA marker gene sequences. *Nature Biotechnology*, 31(9): 814-821. DOI: <https://www.doi.org/10.1038/nbt.2676>
- Lee JS, Wang RX, Goldberg MS, Clifford GP, Kao DJ, and Colgan SP (2020). Microbiota-sourced purines support wound healing and mucous barrier function. *Iscience*, 23(6): 101226. DOI: <https://www.doi.org/10.1016/j.isci.2020.101226>
- Lee KW and Lillehoj HS (2022). Role of *Clostridium perfringens* necrotic enteritis b-like toxin in disease pathogenesis. *Vaccines*, 10(1): 61. DOI: <https://www.doi.org/10.3390/vaccines10010061>
- Lirong H, Meng M, Mingzhu G, Dai C, Lei S, Xu W, and Chunling W (2019). Immunomodulatory activity of a water-soluble polysaccharide obtained from highland barley on immunosuppressive mice models. *Food & Function*, 10(1): 304-314. DOI: <https://www.doi.org/10.1039/c8fo01991f>
- MacCannell AD and Roberts LD (2022). Metabokines in the regulation of systemic energy metabolism. *Current Opinion in Pharmacology*, 67: 102286. DOI: <https://www.doi.org/10.1016/j.coph.2022.102286>
- Morris GF and Mathews MB (1989). Regulation of proliferating cell nuclear antigen during the cell cycle. *Journal of Biological Chemistry*, 264(23): 13856-13864. Available at: <https://pubmed.ncbi.nlm.nih.gov/2569465/>
- Park I, Oh S, Nam H, Celi P, and Lillehoj HS (2022). Antimicrobial activity of sophorolipids against *Eimeria maxima* and *Clostridium perfringens*, and their effect on growth performance and gut health in necrotic enteritis. *Poultry Science*, 101(4). DOI: <https://www.doi.org/10.1016/j.psj.2022.101731>
- Pham VH, Kan L, Huang J, Geng Y, Zhen W, Guo Y, Abbas W, and Wang Z (2020). Dietary encapsulated essential oils and organic acids mixture improves gut health in broiler chickens challenged with necrotic enteritis. *Journal of Animal Science and Biotechnology*, 11: 18. DOI: <https://www.doi.org/10.1186/s40104-019-0421-y>
- Ringnér M (2008). What is principal component analysis?. *Nature Biotechnology*, 26(3): 303-304. DOI: <https://www.doi.org/10.1038/nbt0308-303>
- Simon Á, Jávora A, Bai P, Oláh J, and Czeglédi L (2018). Reference gene selection for reverse transcription quantitative polymerase chain reaction in chicken hypothalamus under different feeding status. *Japanese Journal of Animal Physiology and Animal Nutrition*, 102(1): 286-296. DOI: <https://www.doi.org/10.1111/jpn.12690>
- Skinner JT, Bauer S, Young V, Pauling G, and Wilson J (2010). An Economic analysis of the impact of Subclinical (mild) necrotic enteritis in broiler chickens. *Avian Diseases*, 54(4): 1237-1240. DOI: <https://www.doi.org/10.1637/9399-052110-Reg.1>
- Stanley D, Wu SB, Rodgers N, Swick RA, and Moore RJ (2014). Differential responses of cecal microbiota to Fishmeal, *Eimeria* and *Clostridium perfringens* in a Necrotic enteritis challenge model in chickens. *Plos One*, 9(8): e104739. DOI: <https://doi.org/10.1371/journal.pone.0104739>

- <https://www.doi.org/10.1371/journal.pone.0104739>
- Timbermont L, Haesebrouck F, Ducatelle R, and Van Immerseel F (2011). Necrotic enteritis in broilers: an updated review on the pathogenesis. *Avian Pathology*, 40(4): 341-347. DOI: <https://www.doi.org/10.1080/03079457.2011.590967>
- Timbermont L, Lanckriet A, Dewulf J, Nollet N, Schwarzer K, Haesebrouck F, Ducatelle R, and Van Immerseel F (2010). Control of *Clostridium perfringens*-induced necrotic enteritis in broilers by target-released butyric acid, fatty acids and essential oils. *Avian Pathology*, 39(2): 117-121. DOI: <https://www.doi.org/10.1080/03079451003610586>
- Wade B, Keyburn AL, Seemann T, Rood JI, and Moore RJ (2015). Binding of *Clostridium perfringens* to collagen correlates with the ability to cause necrotic enteritis in chickens. *Veterinary Microbiology*, 180(3-4): 299-303. DOI: <https://www.doi.org/10.1016/j.vetmic.2015.09.019>
- Wang B, Zhou Y, Mao Y, Gong L, Li X, Xu S, Wang F, Guo Q, Zhang H, and Li W (2021a). Dietary supplementation With *Lactobacillus plantarum* ameliorates compromise of growth performance by modulating short-chain fatty acids and intestinal dysbiosis in broilers under *Clostridium perfringens* challenge. *Frontiers in Nutrition*, 8: 706148. DOI: <https://www.doi.org/10.3389/fnut.2021.706148>
- Wang B, Zhou Y, Mao Y, Gong L, Li X, Xu S, Wang F, Guo Q, Zhang H, and Li W (2021b). Dietary supplementation with *Lactobacillus plantarum* ameliorates compromise of growth performance by modulating short-chain fatty acids and intestinal dysbiosis in broilers under *Clostridium perfringens* challenge. *Frontiers in Nutrition*, 8: 706148. DOI: <https://www.doi.org/10.3389/fnut.2021.706148>
- Wang T, Lei H, Zhou L, Tang M, Liu Q, Long F, Li Q, and Su J (2022). Effect of fumonisin B1 on proliferation and apoptosis of intestinal porcine epithelial cells. *Toxins*, 14(7): 471. DOI: <https://www.doi.org/10.3390/toxins14070471>
- Wang Y, Xu Y, Xu S, Yang J, Wang K, and Zhan X (2021c). *Bacillus subtilis* DSM29784 alleviates negative effects on growth performance in broilers by improving the intestinal health under necrotic enteritis challenge. *Frontiers in Microbiology*, 12: 723187. DOI: <https://www.doi.org/10.3389/fmicb.2021.723187>
- Williams RB (2005). Intercurrent coccidiosis, and necrotic enteritis of chickens: Rational, integrated disease management by maintenance of gut integrity. *Avian Pathology*, 34(3): 159-180. DOI: <https://www.doi.org/10.1080/03079450500112195>
- Wu SB, Rodgers N, and Choct M (2010). Optimized necrotic enteritis model producing clinical and subclinical infection of *Clostridium perfringens* in broiler chickens. *Avian Diseases*, 54(3): 1058-1065. DOI: <https://www.doi.org/10.1637/9338-032910-Reg.1>
- Wu SB, Stanley D, Rodgers N, Swick RA, and Moore RJ (2014). Two necrotic enteritis predisposing factors, dietary fishmeal and *Eimeria* infection, induce large changes in the caecal microbiota of broiler chickens. *Veterinary Microbiology*, 169(3-4): 188-197. DOI: <https://www.doi.org/10.1016/j.vetmic.2014.01.007>
- Xiao X (2022). Preliminary studies on the roles of *Clostridium butyricum* for ameliorating gut mucosal barrier of broiler chickens with necrotic enteritis. Tongfang Knowledge Network (Beijing) Technology Co., Ltd. DOI: <https://www.doi.org/10.27409/d.cnki.gxbnu.2022.001409>
- Xie T (2019). Effects of compound acidifier or/and *Radix Bupleurum* extract on growth performance and immune function of broilers challenged with coccidia. DOI: <https://www.doi.org/10.27345/d.cnki.gsnyu.2019.000533>
- Xu K, Wang J, Liu H, Zhao J, and Lu W (2020). Melatonin promotes the proliferation of chicken sertoli cells by activating the ERK/Inhibin alpha subunit signaling pathway. *Molecules*, 25(5): 1230. DOI: <https://www.doi.org/10.3390/molecules25051230>
- Xu S, Lin Y, Zeng D, Zhou M, Zeng Y, Wang H, Zhou Y, Zhu H, Pan K, Jing B et al. (2018). *Bacillus licheniformis* normalize the ileum microbiota of chickens infected with necrotic enteritis. *Scientific Reports*, 8(1): 1744. DOI: <https://www.doi.org/10.1038/s41598-018-20059-z>
- Y HY, S LZ, SL J, L LZ, JW, and M LW (2016). Effects of recombinant epidermal growth factor on the proliferation of the intestinal epithelial cells in early-weaned pigs. *Animal Husbandry & Veterinary Medicine*, 48(4): 70-75. Available at: <https://d.wanfangdata.com.cn/periodical/ChlQZXJpb2RpY2FsO0hJ/TmV3UzlwMjMxMjI2Eg54bXlzeTlwMTYwNDAXNxoIc2doNXI0eXo=>
- Zaytsoff SJM, Montana T, Boras VF, Brassard J, Moote PE, Uwiera RRE, and Inglis GD (2022). Microbiota transplantation in day-old broiler chickens ameliorates necrotic enteritis via modulation of the intestinal microbiota and host immune responses. *Pathogens*, 11(9): 972. DOI: <https://www.doi.org/10.3390/pathogens11090972>
- ZHAN Yuanquan CL, LYU Yonghui, HUANG Yajing, XIE Yingjie, ZHOU Wanfei, and WU Yujin (2022). Effect of Changyanqing on TGF- β 1/Smad3/ERK Pathway in Rats with Ulcerative Colitis. *World Chinese Medicine* 17(14): 1990-1994-2001. Available at: <https://link.cnki.net/urlid/11.5529.r.20220812.1701.004>
- Zhang X, Akhtar M, Chen Y, Ma Z, Liang Y, Shi D, Cheng R, Cui L, Hu Y, Nafady AA et al. (2022a). Chicken jejunal microbiota improves growth performance by mitigating intestinal inflammation. *Microbiome*, 10(1): 107. DOI: <https://www.doi.org/10.1186/s40168-022-01330-y>
- Zhang X, Chen F, He M, Wu P, Zhou K, Zhang T, Chu M, and Zhang G (2022b). miR-7 regulates the apoptosis of chicken primary myoblasts through the KLF4 gene. *British Poultry Science*, 63(1): 39-45. DOI: <https://www.doi.org/10.1080/00071668.2021.1958299>
- Zhao S, Zhang B, Yang J, Zhou J, and Xu Y (2024). Linear discriminant analysis. *Nature Reviews Methods Primers*, 4(1): 70. DOI: <https://www.doi.org/10.1038/s43586-024-00346-y>



Publisher's note: [Scienceline Publication](https://www.scienceline.com) Ltd. remains neutral with regard to jurisdictional claims in published maps and institutional affiliations.

Open Access: This article is licensed under a Creative Commons Attribution 4.0 International License, which permits use, sharing, adaptation, distribution and reproduction in any medium or format, as long as you give appropriate credit to the original author(s) and the source, provide a link to the Creative Commons licence, and indicate if changes were made. The images or other third party material in this article are included in the article's Creative Commons licence, unless indicated otherwise in a credit line to the material. If material is not included in the article's Creative Commons licence and your intended use is not permitted by statutory regulation or exceeds the permitted use, you will need to obtain permission directly from the copyright holder. To view a copy of this licence, visit <https://creativecommons.org/licenses/by/4.0/>.
© The Author(s) 2025